

AD-A014 792

INSTRUMENTED IMPACT TESTING USING A HOPKINSON
BAR APPARATUS

T. Nicholas

Air Force Materials Laboratory
Wright-Patterson Air Force Base, Ohio

July 1975

DISTRIBUTED BY:



AD A 014792

268203

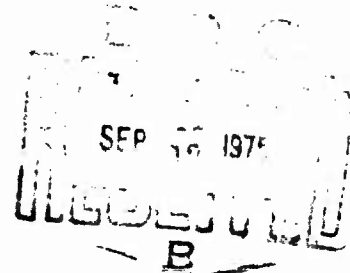
AFML-TR-75-54

INSTRUMENTED IMPACT TESTING USING A HOPKINSON BAR APPARATUS

METALS BEHAVIOR BRANCH
METALS AND CERAMICS DIVISION

JULY 1975

TECHNICAL REPORT AFML-TR-75-54



Approved for public release: distribution unlimited

Reproduced by
NATIONAL TECHNICAL
INFORMATION SERVICE
U.S. Department of Commerce
Springfield, VA 22151

AIR FORCE MATERIALS LABORATORY
AIR FORCE WRIGHT AERONAUTICAL LABORATORIES
Air Force Systems Command
Wright-Patterson Air Force Base, Ohio 45433

NOTICE

When Government drawings, specifications, or other data are used for any purpose other than in connection with a definitely related Government procurement operation, the United States Government thereby incurs no responsibility nor any obligation whatsoever; and the fact that the government may have formulated, furnished, or in any way supplied the said drawings, specifications, or other data, is not to be regarded by implication or otherwise as in any manner licensing the holder or any other person or corporation, or conveying any rights or permission to manufacture, use, or sell any patented invention that may in any way be related thereto.

This report has been reviewed by the Information Office (OI) and is releasable to the National Technical Information Service (NTIS). At NTIS, it will be available to the general public, including foreign nations.

This technical report has been reviewed and is approved for publication.

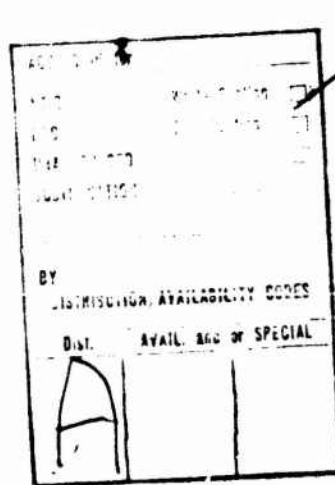


T. Nicholas
Project Scientist

FOR THE COMMANDER



V. J. RUSSO
Chief, Metals Behavior Branch
Metals and Ceramics Division
Air Force Materials Laboratory



Copies of this report should not be returned unless return is required by security considerations, contractual obligations, or notice on a specific document.

UNCLASSIFIED

SECURITY CLASSIFICATION OF THIS PAGE (When Data Entered)

REPORT DOCUMENTATION PAGE		READ INSTRUCTIONS BEFORE COMPLETING FORM
1. REPORT NUMBER AFML-TR-75-54	2. GOVT ACCESSION NO.	3. RECIPIENT'S CATALOG NUMBER
4. TITLE (and Subtitle) INSTRUMENTED IMPACT TESTING USING A HOPKINSON BAR APPARATUS		5. TYPE OF REPORT & PERIOD COVERED
		6. PERFORMING ORG. REPORT NUMBER
7. AUTHOR(s) T. Nicholas, Ph.D.		8. CONTRACT OR GRANT NUMBER(s)
9. PERFORMING ORGANIZATION NAME AND ADDRESS Air Force Materials Laboratory Wright-Patterson Air Force Base, Ohio 45433		10. PROGRAM ELEMENT, PROJECT, TASK AREA & WORK UNIT NUMBERS
11. CONTROLLING OFFICE NAME AND ADDRESS Air Force Materials Laboratory Wright-Patterson Air Force Base, Ohio 45433		12. REPORT DATE July 1975
14. MONITORING AGENCY NAME & ADDRESS (if different from Controlling Office)		13. NUMBER OF PAGES 31
		15. SECURITY CLASS. (of this report) Unclassified
		15a. DECLASSIFICATION/DOWNGRADING SCHEDULE
16. DISTRIBUTION STATEMENT (of this Report) Approved for public release; distribution unlimited.		
17. DISTRIBUTION STATEMENT (of the abstract entered in Block 20, if different from Report)		
18. SUPPLEMENTARY NOTES		
19. KEY WORDS (Continue on reverse side if necessary and identify by block number) Charpy impact Beryllium Hopkinson bar Strain rate		
20. ABSTRACT (Continue on reverse side if necessary and identify by block number) A technique for conducting instrumented Charpy impact tests using a Hopkinson bar is presented. Data for three grades of beryllium covering a range in impact velocities from 20 to 200 in/sec (.5 to 5 m/s) are obtained in the form of load-deflection curves from which maximum load, maximum deflection, and total energy are obtained. Results show good agreement with data on identical materials obtained from an instrumented impact test at 54 in/sec (1.37 m/s) and from a standard Charpy impact machine at 135 in/sec (3.43 m/s). The advantages and limitations of the Hopkinson bar apparatus are discussed.		

TABLE OF CONTENTS

SECTION	PAGE
I INTRODUCTION	1
II APPARATUS AND INSTRUMENTATION.	3
III EXPERIMENTAL RESULTS	7
IV DATA FOR BERYLLIUM	10
V DISCUSSION AND CONCLUSIONS	12
REFERENCES	17

Preceding page blank

LIST OF ILLUSTRATIONS

FIGURE	PAGE
1. Schematic of Apparatus and Instrumentation	19
2. Data Reduction Schematic	20
3. Geometry of Specimen and Fixture	21
4. Typical Oscilloscope Photographs	22
5. Energy as a Function of Impact Velocity	23
6. Maximum Load versus Impact Velocity	24
7. Maximum Deflection versus Impact Velocity	25
8. Typical Load-Deflection Curves for P-1 Beryllium	26
9. Uniaxial Stress-Strain Curves for Beryllium	27

LIST OF TABLES

TABLE	
1. Beryllium Chemical Analysis	18

SECTION I

INTRODUCTION

Structural applications involving dynamic or impulsive loading present unique problems for the materials engineer. In addition to the demand for design data for materials at high rates of strain, there is the necessity for a screening test to determine the acceptability of a material on a batch to batch basis. For designs and applications where the dynamic response is a critical aspect of the materials behavior, a screening test should involve high rates of strain comparable to those which may be encountered in service. In addition to these requirements, economics dictates that the screening test be easy to perform, the apparatus be readily available, and the test specimen be as simple as possible. Above all else, however, it is important that the screening test data be meaningful as related to the structural application. Thus, thin gage materials should be tested in thin gage form; materials subjected to tension should be tested in tension, etc.

The Charpy impact test is one of the screening tests that comes close to meeting this list of requirements for materials in dynamic structural applications. For materials with limited ductility, and thus low impact energy, the standard Charpy test is sometimes difficult to perform because of the very low energy absorbed and the resulting poor experimental accuracy. To overcome this, instrumented impact testing appears to offer a rational solution. Turner (Ref. 1) presents a summary review of instrumented Charpy impact testing. Instead of

obtaining energy from the height of a pendulum swing, this test offers the possibility of obtaining the complete load-time history of the impacted specimen.

Sophisticated versions of the instrumented impact test (Ref. 2) allow a load-time trace to be obtained for a (nominally) constant impact velocity as well as an electronically integrated signal which is proportional to energy absorbed in the specimen. For specimens with low ductility, measurement accuracy is not sacrificed because of the flexibility of altering the time base of the recording system for optimum time resolution.

Among the questions that arise, however, in the use of an instrumented Charpy impact test is the accuracy of the load measuring system under impact conditions. The load on the specimen is sensed via strain gages mounted on the sides of the impacting "tup". Since the gages are some finite distance from the point of contact and the tup is part of a more rigid structure consisting of the pendulum and the mounting mechanism, wave reflections and interactions from the various free and fixed boundaries would appear to play some part in the signals recorded with the strain gages. As the total time of the test becomes shorter for a more brittle material, the question arises as to how important wave reflections might be in the interpretation of experimental data from an instrumented Charpy impact test. In addition, the energy absorbed by the vibration and elastic energy of the impacting machine must be considered (Ref. 2). Finally, the inertia of the specimen must be considered and corrected for (Refs. 3, 4, and 5). The interpretation

of load-time records from instrumented impact tests has been shown to be rather critical when brittle materials are tested (Ref. 1). Factors such as the inherent electronic limitations can also play an important role in interpretation of data from an instrumented impact test (Ref. 2).

To answer some of these questions, and to investigate the applicability of instrumented impact testing to beryllium, an investigation was undertaken to determine the notched bend behavior of beryllium at high impact velocities using a modification of a Hopkinson bar apparatus. A description of the apparatus and instrumentation and experimental data on load, deflection, and energy covering an order of magnitude in impact velocity are presented for several structural grades of beryllium. The results are compared with instrumented impact test data obtained using a Dynatup system and data from a Phymet Charpy impact machine. The advantages and limitations of the Hopkinson bar technique are delineated.

SECTION II

APPARATUS AND INSTRUMENTATION

The apparatus used in this investigation, consisting principally of a striker bar, an input bar, and a support fixture, is shown schematically in Fig. 1. The so-called Hopkinson bar apparatus is used in the manner originally conceived by B. Hopkinson (Ref. 6) as a method of deducing what happens at the end of a bar through observations farther down the bar. In this setup, the complete force-time and displacement time histories at the end of the bar in contact with the specimen can be

determined from observations of the pulse propagating down the bar and then later reflecting from the specimen, utilizing a strain gage bridge at the center of the incident bar. The pulse which loads the specimen is generated through the impact of the striker bar which is accelerated against the incident bar using a torsional spring arrangement to store and then suddenly release energy, the amplitude of the incident pulse being proportional to the impact velocity (Ref. 7). The time duration or length of the pulse is twice the wave transit time in the striker bar. For the steel striker bar of length 48 in., (1.22 m) the incident pulse is approximately 500 μ sec in duration. The pulse which propagates down the input bar is recorded with the aid of a strain gage bridge, the recorded strain-time history providing a complete record of the strain, stress, and particle velocity histories which occur some time later at the end of the bar in contact with the specimen. The time difference of the recording of the incident pulse travelling to the right with the strain gages and the actual event at the end of the bar is the longitudinal wave transit time from the gages to the end of the bar. It is assumed in the analysis that the pulses in the bar are purely elastic and travel in a non-dispersive manner at the elastic bar velocity which is determined experimentally. When the incident pulse arrives at the specimen, part of it is reflected and part transmitted into and through the specimen into the rigid support fixture. The stress, strain, and particle velocity associated with the leftward travelling reflected pulse are recorded some time later at the strain gage bridge at the center of the input bar. The time delay between event and recording is, again, the wave transit time between the end of the

bar and the gages. The net stress, strain, and particle velocity at the specimen are the sum of the individual contributions of the incident and reflected pulses.

The data reduction for the test is depicted schematically in Fig. 2. By shifting the incident and reflected stress pulses by an amount τ , which is twice the wave transit time between the gages and the end of the bar, the pulses appear to be time coincident as shown in Fig. 2b. Denoting the incident compressive pulse as ϵ_i and the time shifted reflected pulse as ϵ_r (tension positive), the net force at the specimen is then

$$F_s = EA(\epsilon_i - \epsilon_r) \quad (1)$$

where E is Young's modulus and A the cross-sectional area of the input bar. The net particle velocity at the end of the bar is

$$v_s = c(\epsilon_i + \epsilon_r) \quad (2)$$

where c is the elastic bar velocity. The displacement at the end of the bar is then easily obtained by integrating Eq. (2) with respect to time.

$$\delta_s = c \int_0^t (\epsilon_i + \epsilon_r) dt \quad (3)$$

All data are recorded on a dual beam oscilloscope with the aid of a Polaroid camera. A circuit which generates a rectangular pulse upon contact of the striker bar with the input bar is used to trigger the electronics. The pulse generated can be delayed with respect to the time of contact in addition to the width being adjustable. The first beam of the dual beam scope is triggered off the front of the rectangular pulse which has been delayed by an amount equal to the wave transit time

from the striker end of the bar to the strain gage bridge. The second beam on the scope, which records the reflected pulse, is triggered off the back of the rectangular pulse, the width of the pulse having been accurately adjusted to coincide with twice the wave transit time from gages to specimen. The length of the striker bar is less than half the length of the input bar so that the entire incident pulse is past the strain gage bridge before the first of the reflected pulse arrives at the bridge. The striker bar is of the same material and cross-sectional area as the input bar to insure that only a single pulse is generated upon contact and no other spurious pulses occur to interfere with the recording of the incident and reflected pulses.

The wave speed, c , in the input bar is determined experimentally by measuring the time required for a pulse to reflect back and forth in the bar several times. Pulses from a time mark generator are superimposed on the oscilloscope display using the chopped mode of the pre-amplifier for an accurate time base. The mass density of the bar, ρ , is determined experimentally by weighing and measuring the bar accurately. The elastic or Youngs modulus is then calculated from

$$E = \rho c^2 \quad (4)$$

The strain gage bridge on the incident bar is calibrated by measuring the impact velocity of the striker bar and calculating the resulting strain amplitude from the elastic wave propagation equations. An alternate calibration scheme involves shunting a known calibration resistor across one arm of the bridge. The accuracy of this calibration depends, however, on the accuracy of the gage factor given by the

manufacturer and the assumption that static and dynamic calibrations are identical. The velocity measuring scheme was felt to be more reliable and was used exclusively in these experiments.

The geometry of the loading fixture is that of the standard ASTM E23 Charpy impact test loading head (Ref. 8), shown in Fig. 3. The loading head is machined out of a piece of bar of the same material and cross-sectional area as the Hopkinson input bar. The bar is cut off where the 30° taper meets the original circular cross section, making a loading tup of approximately the same length as the diameter of the input bar. The top is attached to the input bar with epoxy cement to hold it in place. Since the joint sees essentially only net compressive stresses, the strength of the joint is not critical. The very thin epoxy joint has no effect on the propagating pulses although the taper introduces small amounts of dispersion into the pulses.

SECTION III

EXPERIMENTAL RESULTS

Three grades of beryllium were subjected to impact tests using the modified Hopkinson bar apparatus. The specimens were machined and etched to the final dimensions shown in Fig. 3. A U-notch was chosen for beryllium because of the relatively low energy absorbed in a Charpy impact test and because of the difficulty and expense in putting fatigue cracks in beryllium specimens. The notches were machined using an electro discharge machining technique. The specimens were etched approximately .004"-.005" (.102-.127 mm) per surface to remove any residual machining

damage. The specimens were all cut from solid cylindrical billets with the axis of the notch parallel to the axis of the cylinder. Two grades of hot isostatically pressed (HIP) beryllium, P-1, and P-10, from Kawecki Berylco Industries (KBI) and one grade of hot-pressed block beryllium, S-65, from Brush-Wellman, Inc. (BW) were tested in this program. The chemistries as supplied by the manufacturers are presented in Table 1.

Two different input bar diameters, .750" and .485", (19.0 and 12.3 mm) were used to achieve a range in input velocities covering an order of magnitude from approximately 20 to 200 in/sec (.5 to 5 m/s). One limitation of the resultant specimen velocity range is the experimental accuracy obtainable when adding and subtracting separate pulse magnitudes (see Eqs. 1 and 3). Since the force required to break the specimen is a function of the material being tested and thus cannot be altered, the input pulse should have a corresponding force level sufficient to break the specimen but not too large to lose accuracy when subtracting the reflected pulse amplitude to obtain force in the specimen from Eq. (1). The particle velocity can only be increased for a specific input force level by decreasing the cross-sectional area of the bar, i.e., by increasing the strain input; thus, the smaller the diameter of the bar, the larger the input strain to achieve the same input force. Note also that the signal-to-noise level on the strain gage output decreases as the signal decreases, thus limiting the lower end of effective input velocities. In addition, the total time of the input pulse is fixed by the length of the striker bar. As the input velocity decreases, the time to failure increases for a specific deflection to failure but cannot exceed the time duration of the input pulse.

Following a trial and error procedure in which it was attempted to maintain reasonable experimental accuracy, a range in input velocities from 20 to 200 in/sec (.5 to 5 m/s) could be obtained for the beryllium samples using the two different diameter input bars. Typical pulses are shown in Fig. 4 for three different velocities. The traces in (a) are obtained with the larger diam. bar, the other two with the smaller bar. The data were reduced in accordance with Eqs. (1) to (3) digitally using a Hewlett Packard Model 9820A Calculator, digitizer, and plotter system. Numerical integration using a trapezoidal rule was performed to obtain the displacements from Eq. (3) and to calculate the energy from the resultant load-deflection traces obtained from a series of time coincident load and displacement values.

Energy as a function of impact velocity for the three materials is presented in Fig. 5. Impact velocity was taken as the value at the point of failure (at maximum load). The average velocity, which varies throughout the test, is somewhat higher than the value quoted for each test. Maximum load and maximum deflection to failure are presented in Figs. 6 and 7 as a function of impact velocity. Typical load-deflection curves are shown in Fig. 8 for P-1 beryllium at three different impact velocities corresponding to those of Fig. 4. At the highest velocity shown of 121 in/sec (3 m/s), oscillations are a predominant feature of the load-deflection curve obtained from the original traces shown in Fig. 4(c). At higher velocities, the oscillations in the reduced load-deflection curves become even more pronounced. The lower velocity of 18 in/sec (.5 m/s) was obtained using the large diameter input bar; the higher velocities using the smaller bar.

In addition to the data obtained using the Hopkinson bar apparatus, several data points are presented which were obtained using two other test methods. Results from instrumented Charpy impact tests using a Dynatup system were performed on specimens of each of the three grades of beryllium from the same lots used in the Hopkinson bar tests. The impact velocity, which is nearly constant in the Dynatup test, was 54 in/sec (1.37 m/s). The tests were all conducted at Union Carbide Corp., Linde Division (Ref. 9) using a Charpy impact machine of 17.6 ft-lb (23.9J) capacity. A second series of Charpy impact tests were performed on a Phymet Charpy impact test machine of 25 ft-lb (34J) capacity. The energy values were determined to an accuracy of approximately $\pm .03$ ft-lb (.04J) on this machine with an impact velocity of 135 in/sec (3.43 m/s). Again, specimens of all three materials were from the same lots as the other tests. The Dynatup and Phymet data are shown on the energy plot in Fig. 5. Dynatup data for maximum load and displacement are also shown in Figs. 6 and 7.

SECTION IV

DATA FOR BERYLLIUM

Energy to failure, maximum load, and maximum deflection are shown as a function of impact velocity in Figs. 5, 6 and 7, respectively, for the three grades of beryllium tested. It can be seen from all three plots that there is no significant change in any of the three measured material parameters with impact velocity over an order of magnitude in velocity as obtained with the Hopkinson bar apparatus. The energy plot shows S-65

to have the highest impact energy, P-1 the next highest, and P-10 the lowest among the three grades of beryllium tested within the velocity range covered. The plot of maximum load versus energy, Fig. 6, shows very little significant difference in maximum load to failure for the three different materials. The P-1 beryllium appears to be consistently higher than the S-65 or P-10 grades, although the difference is slight and is obscured to a large extent by the sample to sample variation in each material. The maximum deflection plot, Fig. 7, shows the same ranking as the energy plot with S-65 highest, P-1 next, and P-10 lowest.

For comparison, typical quasi-static uniaxial stress-strain curves are shown in Fig. 9 along with average values of tensile elongation to failure and ultimate tensile strength. The average values are based on ten tests of each material from the same billet as the impact samples were obtained. The tensile bars were taken with their axes in the transverse direction; i.e. normal to the axis of the cylindrical billet. This direction coincides with that across the notch in the impact specimens and corresponds to the direction of highest elongation in these materials for the shapes of billets fabricated. The material with the highest average tensile elongation in the transverse direction, S-65, also had the largest deflection and greatest impact energy. The ranking of materials based on tensile elongation was consistent with the ranking from the impact test although it is important to note that the two tests are performed at considerably different loading rates. Although the uniaxial ultimate tensile strength of S-65 beryllium is approximately twenty percent less than the other two grades, the maximum load in the

impact test was only slightly lower than the P-1 and comparable to that of the P-10 (see Fig. 6). Because of the complex stress state around a notch in bending it is difficult to draw conclusions regarding the failure criterion in bending in the presence of a stress concentration under impact loading as related to uniaxial stress-strain behavior.

SECTION V

DISCUSSION AND CONCLUSIONS

The Hopkinson bar technique allows one to obtain complete load-time histories in a Charpy impact test over a range in impact velocities covering an order of magnitude. The experimental accuracy depends on the errors introduced in adding and subtracting two electronic signals from a strain gage bridge which have been shifted to appear to be time coincident. It is critical that the time shifting of the pulses be accurate and reproducible. In the experiments performed here using the electronic triggering described, the time shift was accurate to within approximately two microseconds. Times to failure in the experiments ranged from a high of 500 μ sec, the entire length of the input pulse, to a low of under 50 μ sec at the highest impact velocities.

The principle advantage of this technique is that the data represent the true forces and displacements at the end of the bar in contact with the specimen. The only assumptions are that the supporting fixture is rigid and that the pulses propagate in a purely non-dispersive manner down the bar. In preliminary experiments using no specimen at all, the input and reflected pulses could not be distinguished from one another.

other than for the change in sign from the input compression to the reflected tension. By the time the incident pulse has reached the strain gage bridge it has been rounded off to a risetime of approximately $10 \mu \text{ sec}$. Transients having risetimes much less than $10 \mu \text{ sec}$ will thus be expected to be obscured through dispersion as they travel down the bar from the specimen impact end to the gages. There is, however, no problem in interpreting or approximating machine deflection or compliance in this type of test. The pulses show exactly what is happening at the end of the bar subject only to the approximations mentioned and within the experimental and data reduction accuracy.

Another advantage of this technique is the ability to calibrate the system dynamically. The use of a striker bar of the same material and cross-sectional area as the input bar allows direct dynamic calibration of the strain gage signal through a measurement of striker bar velocity. It is not necessary to use a standard specimen of some reference material as is done in calibrating instrumented impact machines. Thus, machine compliance and oscillations do not have to be considered or corrected for in this technique.

The limitations of the test are related to the accuracy available because of the necessity of both adding and subtracting pulses which have been shifted in time. Since experimental accuracy is usually some percentage of full scale, if both pulses are of nearly the same magnitude the difference between the two, proportional to specimen load from Eq. (1), will be of much lower accuracy than that of the individual pulses. On the other hand, if the reflected pulse is very small compared

to the input pulse, the sum of the two will be almost as accurate as the input pulse itself and the difference will still be quite accurate. It is thus desirable to have a reflected pulse which is small with regard to the input pulse. This would require the input force to be only slightly higher than the force in the specimen and would, in turn, cause large variations in velocity in the specimen since the amount of energy available to deform the specimen would be minimal. There are thus many tradeoffs to be made in choosing the size of input bar based on the velocities required and the strength of the specimen to be tested.

For the beryllium specimens tested in this program, reliable and reasonably accurate data could be obtained at input velocities from approximately 20 to 60 in/sec (.5 to 1.5 m/s) using a .75" (19.0 mm) diam input bar and from 50 to 100 in/sec (1.25 to 2.5 m/s) using a .485" (12.3 mm) diam bar. Higher velocities could be obtained but the problems of inertia forces in the Charpy three point bend specimens start to become important. (See Figs. 4 and 8) The load-deflection curve in Fig. 8(c) obtained at an input velocity of 121 in/sec (3 m/s) shows significant inertia forces and oscillations of the test specimen. As the velocities are increased, the inertia forces and oscillations become more pronounced and start to obscure the true material behavior. Comparison of the load-deflection curves of Fig. 8 with a typical load-time trace from an instrumented impact test as shown in Fig. 4 of Ref. 2 shows that oscillations and inertia loading are considerably more troublesome in the instrumented impact test than for similar velocities in the Hopkinson bar tests described herein. The reason for this is that the specimen is impacted directly by a moving hammer in the Charpy test whereas the Hopkinson bar

is already in contact with the specimen and transmits a stress pulse which has a finite risetime of approximately 10μ sec, thereby softening the initial shock.

An attempt was made to quantify the inertia forces in the beryllium specimens experimentally using the Phymet impact machine. Broken beryllium specimens were put together with a piece of tape on the loaded side opposite the notch. The specimen was then tested and the energy recorded. Based on five tests, a value of .06 ft-lb (.08J) was obtained at a corresponding velocity of 135 in/sec (3.43 m/s). A constant acceleration of the specimen as a rigid body for 10μ sec up to the final velocity gives a calculated acceleration force of approximately 750 lb. (3.34 KN) and a corresponding energy of .045 ft-lb (.06J). It can thus be seen that acceleration forces can become significant at these impact velocities and would tend to obscure the origin of the load-time history of the specimen even though the energies involved in accelerating the specimen are not too significant, i.e. under ten percent of the total energy absorbed.

The Hopkinson bar technique is also limited in the total time during which energy is available to fracture the specimen. For the 48" (1.22 m) length of striker bar used here and a 120" (3.05 m) input bar, the total width of the incident pulse is 500μ sec. If the average strength of a specimen of a structural material is assumed to be 2000 lb (8.9 KN), the total energy absorbed at an average velocity of 100 in/sec (2.5 m/s) is 8.3 ft-lb (11.3J). The technique is thus limited to materials with limited amounts of ductility unless higher velocities and/or longer bars

are used. If a maximum average velocity of 100 in/sec (2.5 m/s) is used, corresponding to the limit up to which oscillations in the traces are not significant, then a maximum specimen deflection of .05" (1.25 mm) could be obtained within the maximum 500 μ sec time period of this test.

The agreement between the Hopkinson bar data and the data from two other techniques for a material with as low an impact energy as beryllium is quite good. The values of energy from the Hopkinson bar, Dynatup, and Phymet machines as shown in Fig. 5 are all consistent within the scatter from sample to sample for each of the three materials tested. The values for maximum load, Fig. 6, appear to be somewhat lower for the Dynatup data compared to the Hopkinson bar data. Deflection data in Fig. 7, on the other hand, appear to be consistent. Note, again, the limited accuracy in reducing data of this type because of oscillations which tend to obscure the true load deflection behavior of the material. From the data obtained in this investigation it can be concluded that the assumptions, corrections, and accuracy of the three techniques are comparable. The ability to duplicate Dynatup instrumented impact data indicates that the data reduction procedures for instrumented impact testing appear to be confirmed. The data from the Phymet machine provided a valuable cross check on the other two procedures while also demonstrating that low impact energy materials can be tested on that type of machine if maximum load and deflection are not required.

REFERENCES

1. C.E. Turner, "Measurement of Fracture Toughness by Instrumented Impact Test," Impact Testing of Materials, ASTM STP 466, American Society for Testing and Materials, 93-114, 1970.
2. D.R. Ireland, "Procedures and Problems Associated with Reliable Control of the Instrumented Impact Test," Instrumented Impact Testing, ASTM STP 563, American Society for Testing and Materials, 3-29, 1974.
3. J.C. Radon and C.E. Turner, "Fracture Toughness Measurements by Instrumented Impact Test," Engr. Fracture Mech., 1, 411-428 (1969).
4. H.J. Saxton, D.R. Ireland, and W.L. Server, "Analysis and Control of Inertial Effects During Instrumented Impact Testing," Instrumented Impact Testing, ASTM STP 563, American Society for Testing and Materials, 50-73, 1974.
5. S. Venzi, A.H. Priest, and M.J. May, "Influence of Inertial Load in Instrumented Impact Tests," Impact Testing of Metals, ASTM STP 466, American Society for Testing and Materials, 165-180, 1970.
6. B. Hopkinson, "A Method of Measuring the Pressure Produced in the Deformation of High Explosives or by the Impact of Bullets," Phil. Trans. Roy. Soc., A, 213, 437-456 (1914).
7. U.S. Lindholm, "Some Experiments with the Split Hopkinson Pressure Bar," J. Mech. Phys. Solids, 12, 317-335 (1964).
8. "Notched Bar Impact Testing of Metallic Materials," ASTM Standards E23-72, 1972 Annual Book of ASTM Standards, American Society for Testing and Materials, 276-292, 1972.
9. Dr. Thomas A. Taylor, Union Carbide Corp., Linde Division, personal communication.

Table 1
Beryllium Chemical Analysis (PPM)

<u>Element</u>	<u>BW S-65</u>	<u>KBI P-1</u>	<u>KBI P-10</u>
Al	190	40	340
C	250	120	800
Cr	60	20	60
Cu	40	20	35
Fe	580	280	950
Mn	20	8	160
Ni	40	100	85
Si	170	60	160
Ti	100		
Mg	-20	10	180
BeO(%)	.53	.97	1.11

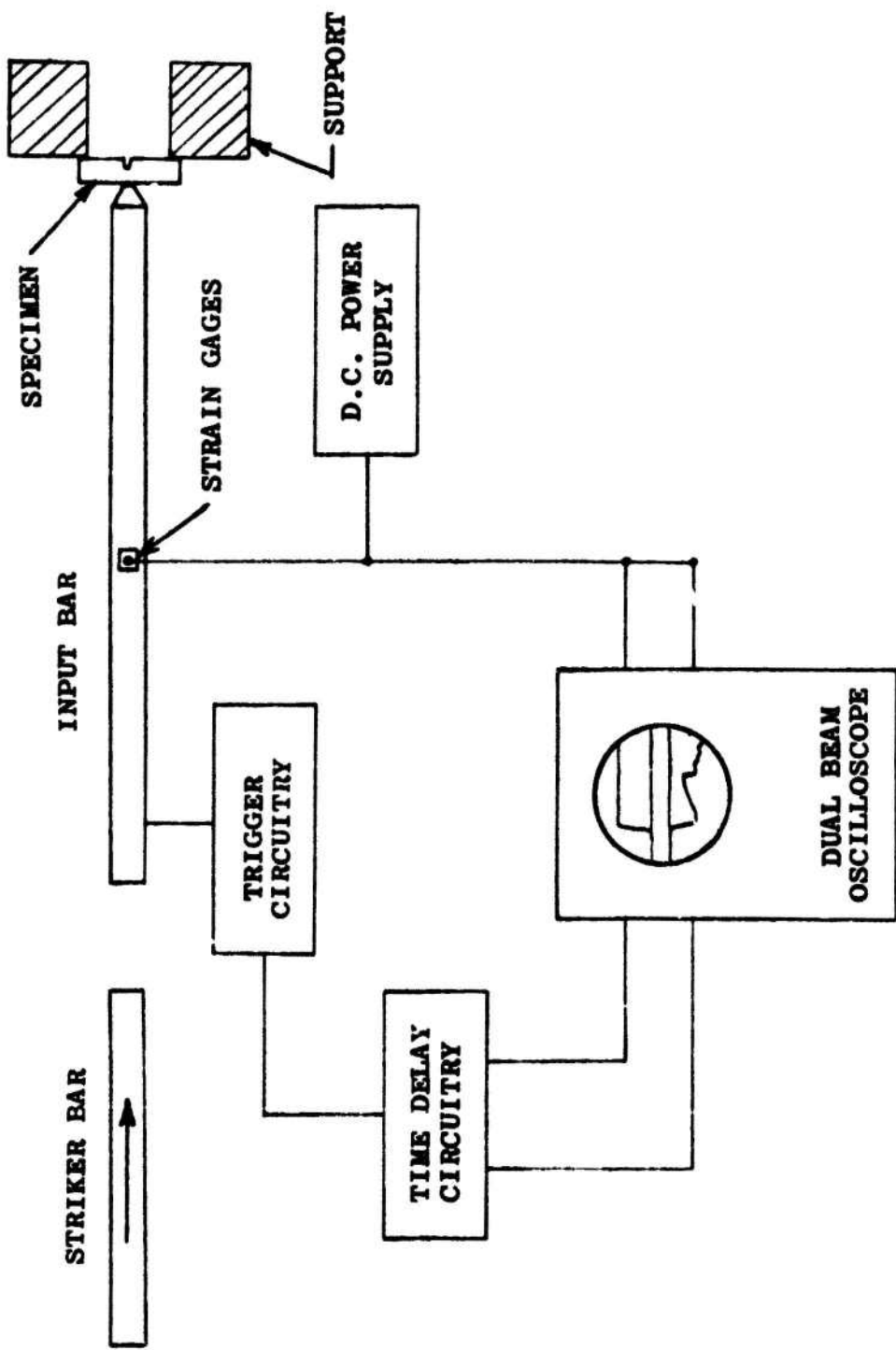


Figure 1. Schematic of Apparatus and Instrumentation.

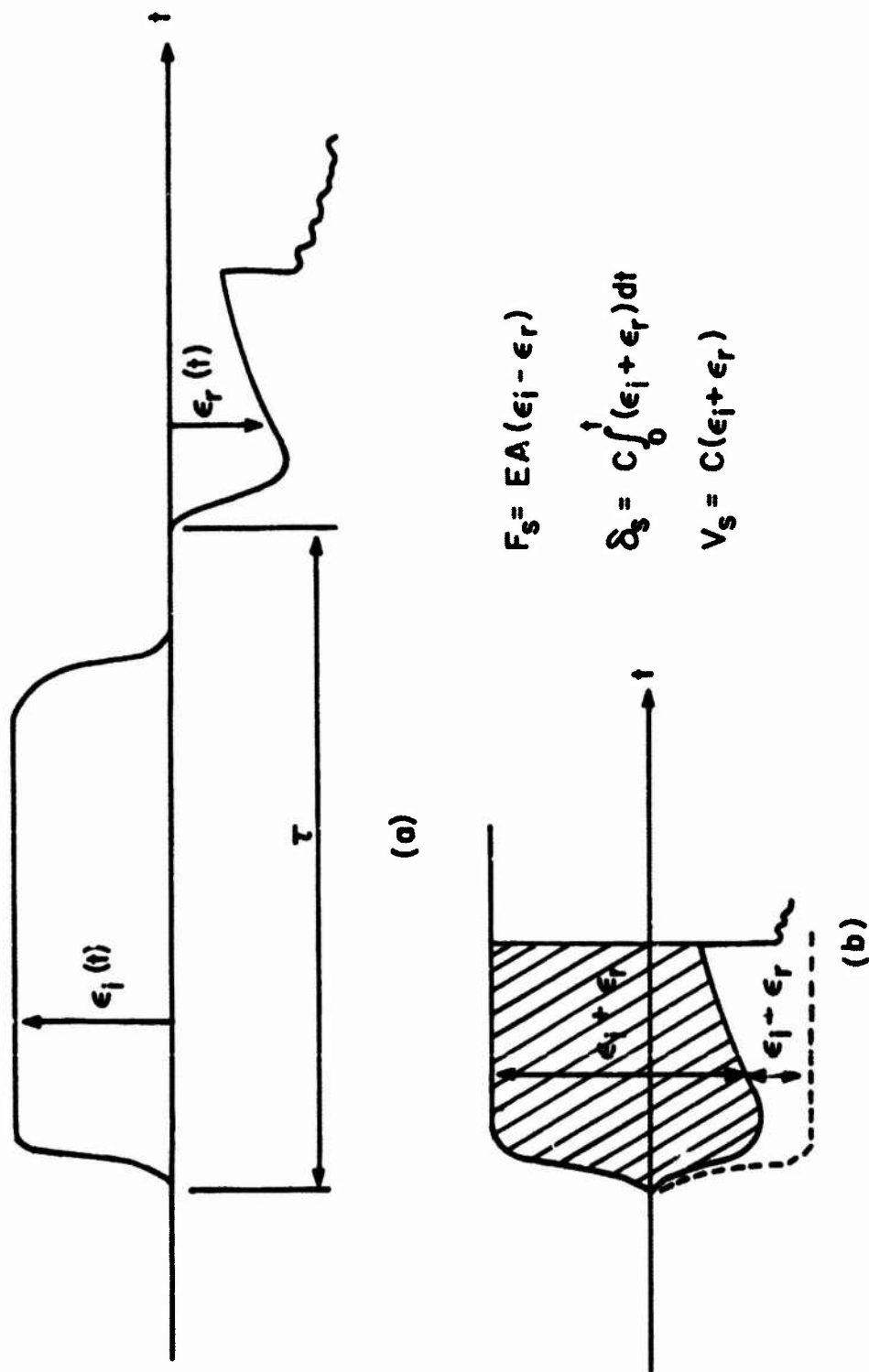


Figure 2: Data Reduction Schematic

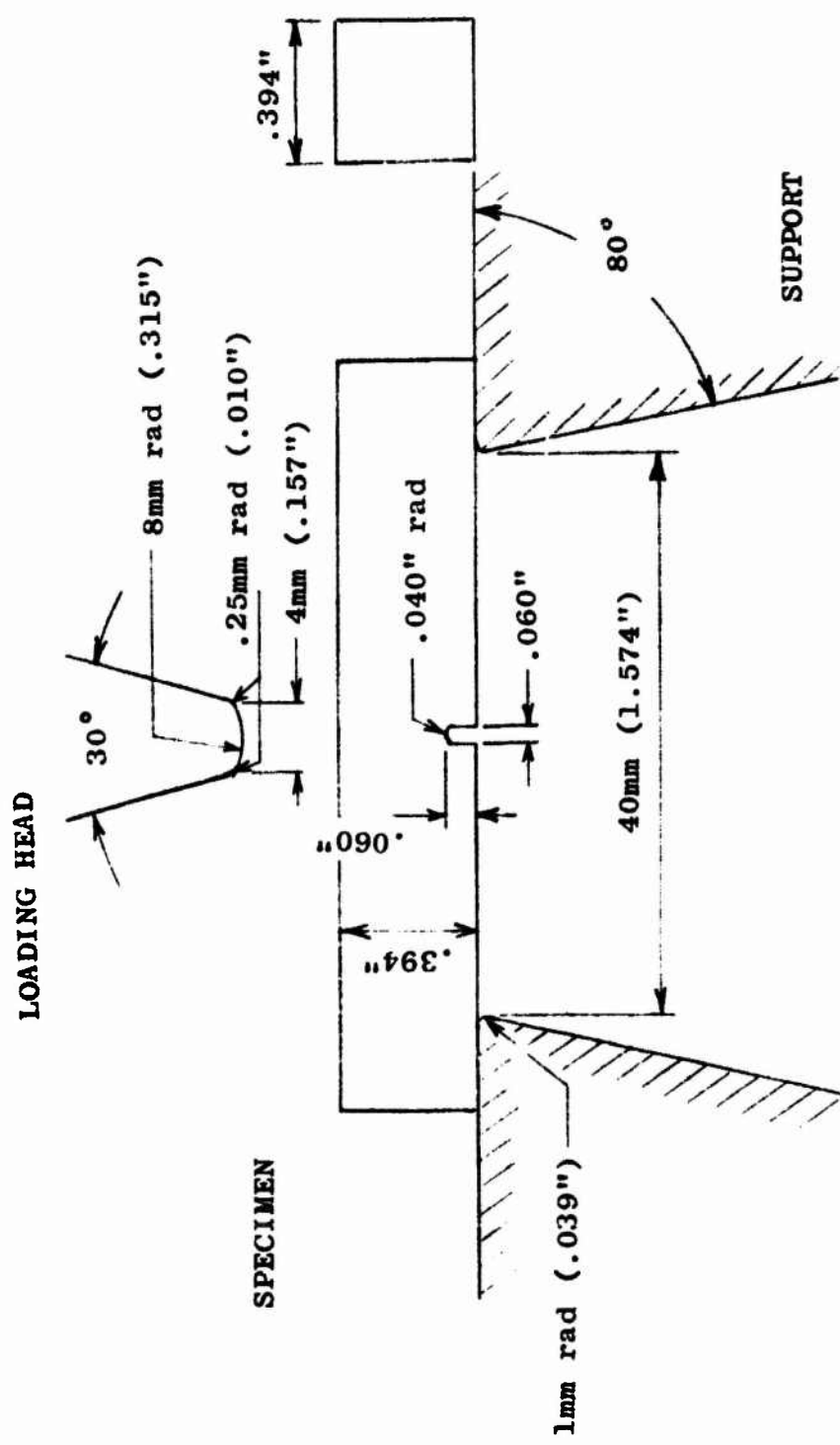
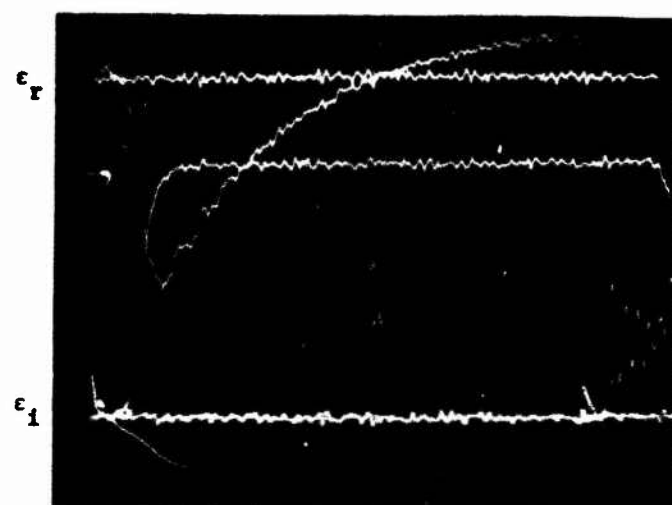


Figure 3. Geometry of Specimen and Fixture



Vert. $25.3 \mu\text{e}/\text{div}$

Horiz. $50 \mu\text{sec}/\text{div}$

18 in/sec

(a)

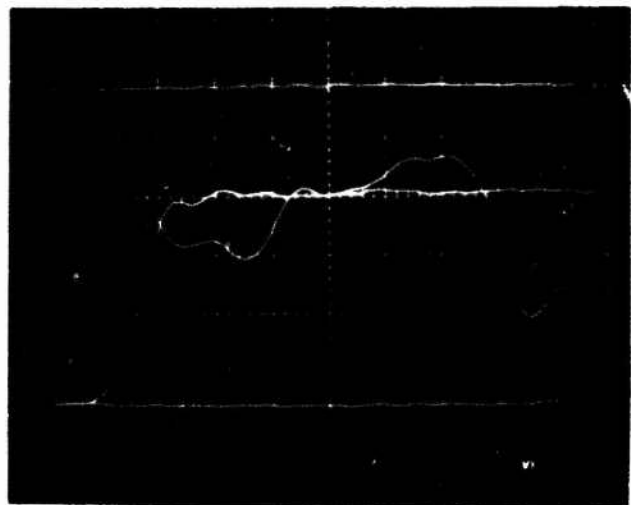


Vert. $126 \mu\text{e}/\text{div}$

Horiz. $20 \mu\text{sec}/\text{div}$

96 in/sec

(b)



Vert. $126 \mu\text{e}/\text{div}$

Horiz. $10 \mu\text{sec}/\text{div}$

121 in/sec

(c)

Figure 4. Typical Oscilloscope Photographs. a) .75" diam bar,
 $E = 29.66 \times 10^6 \text{ psi}, c = 2.02 \times 10^5 \text{ in/sec}$; b,c) .485" diam bar,
 $E = 30.70 \times 10^6 \text{ psi}, c = 2.04 \times 10^5 \text{ in/sec}$.

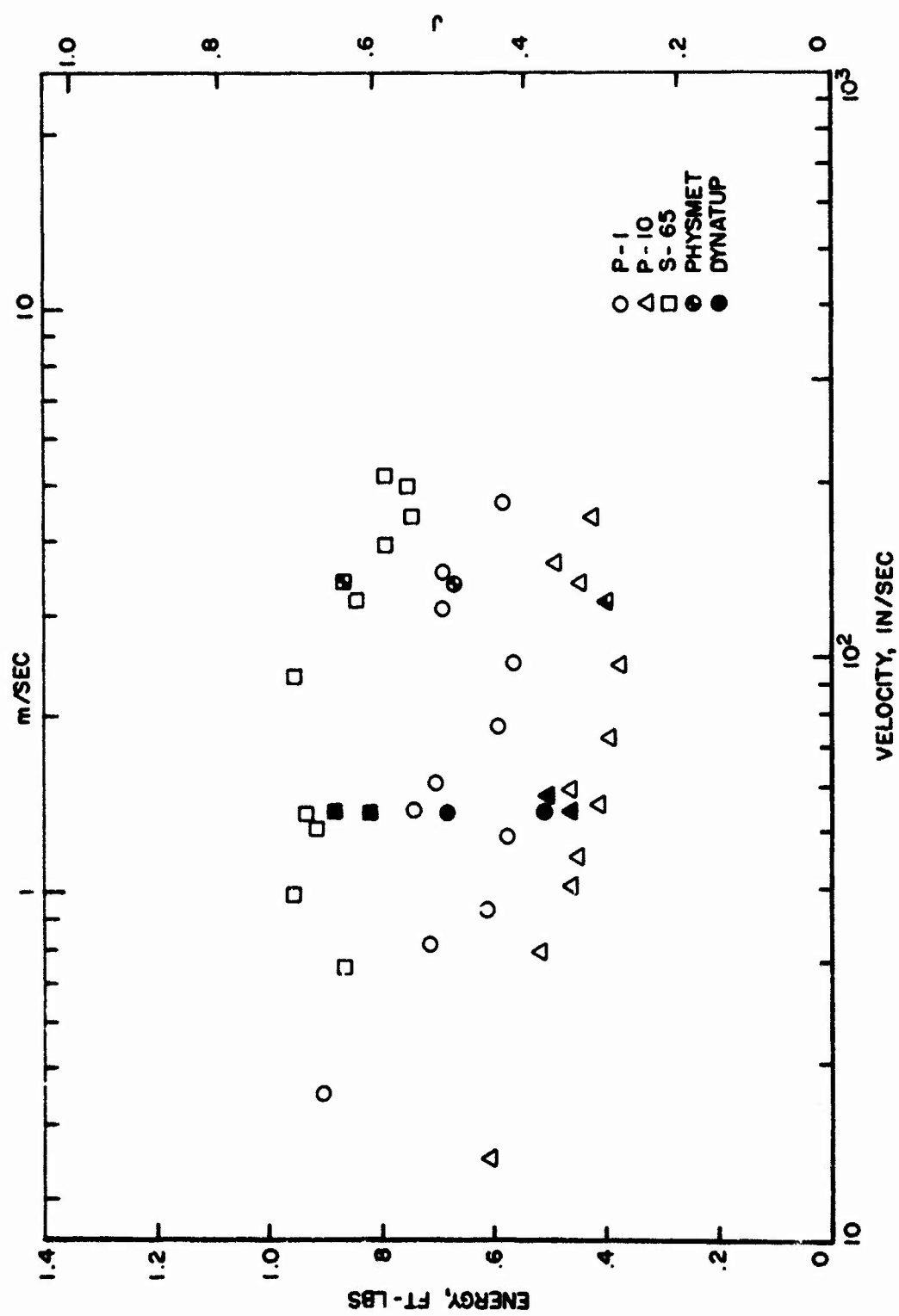


Figure 5. Energy as a Function of Impact Velocity

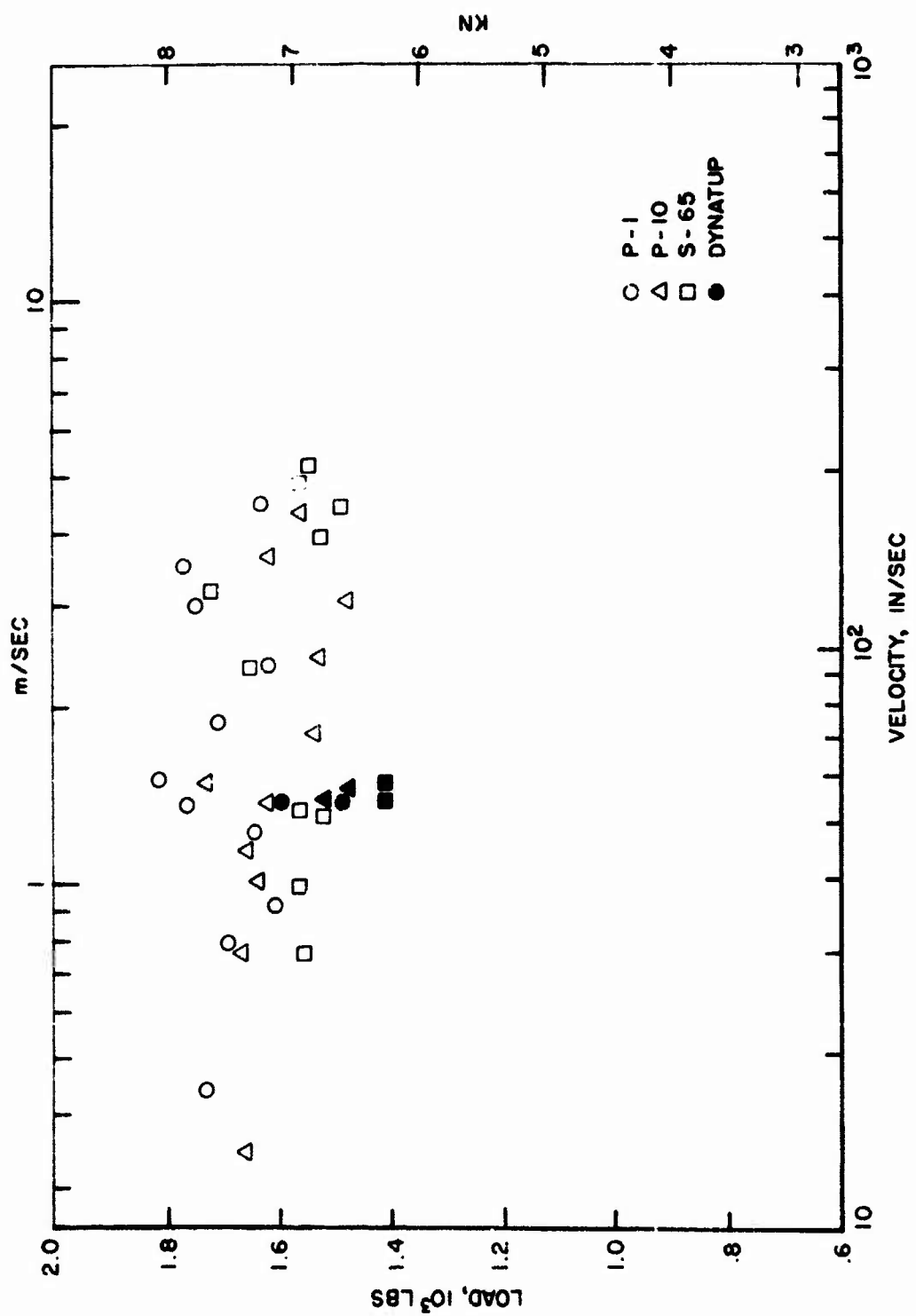


Figure 6. Maximum Load versus Impact Velocity

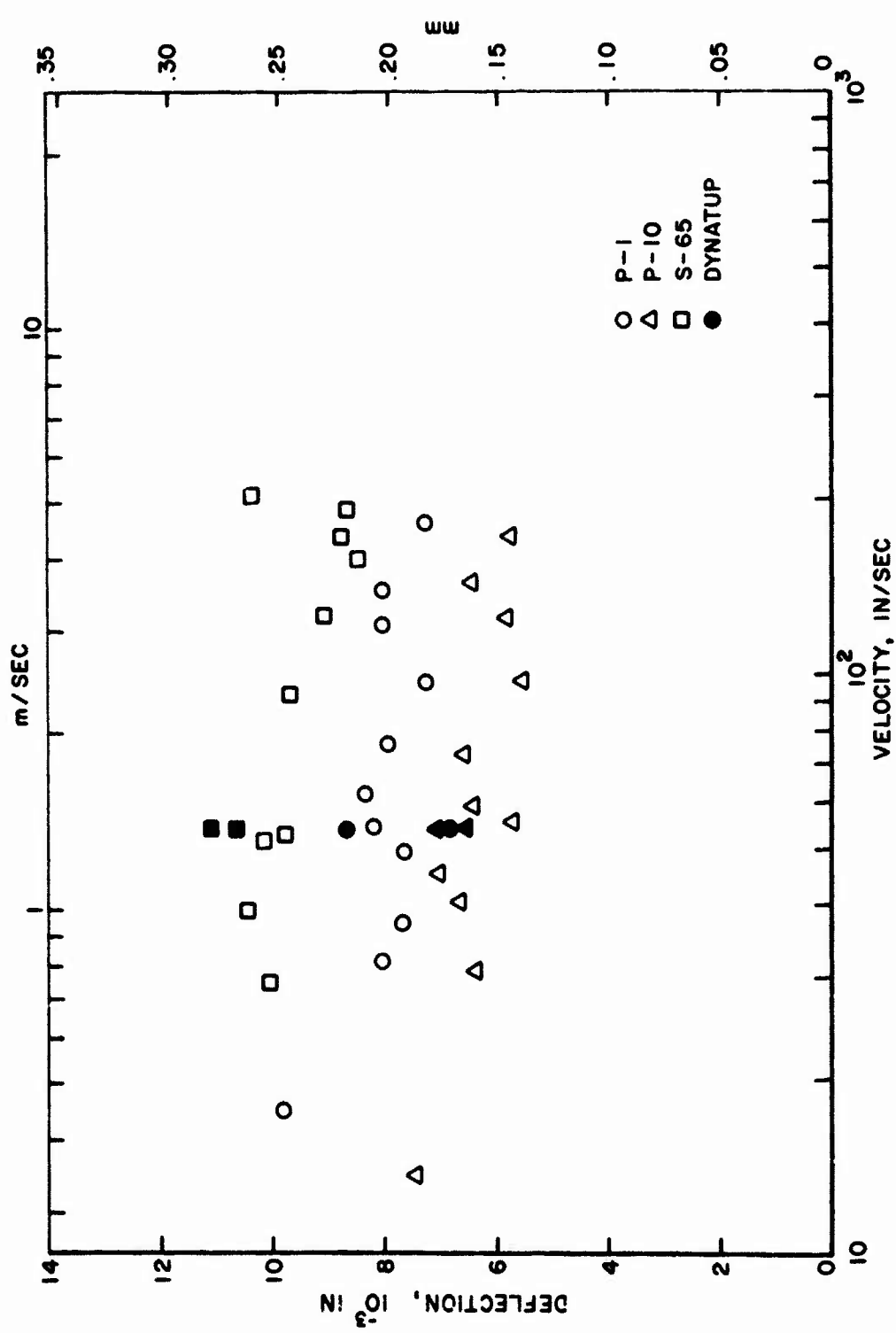


Figure 7. Maximum Deflection versus Impact Velocity

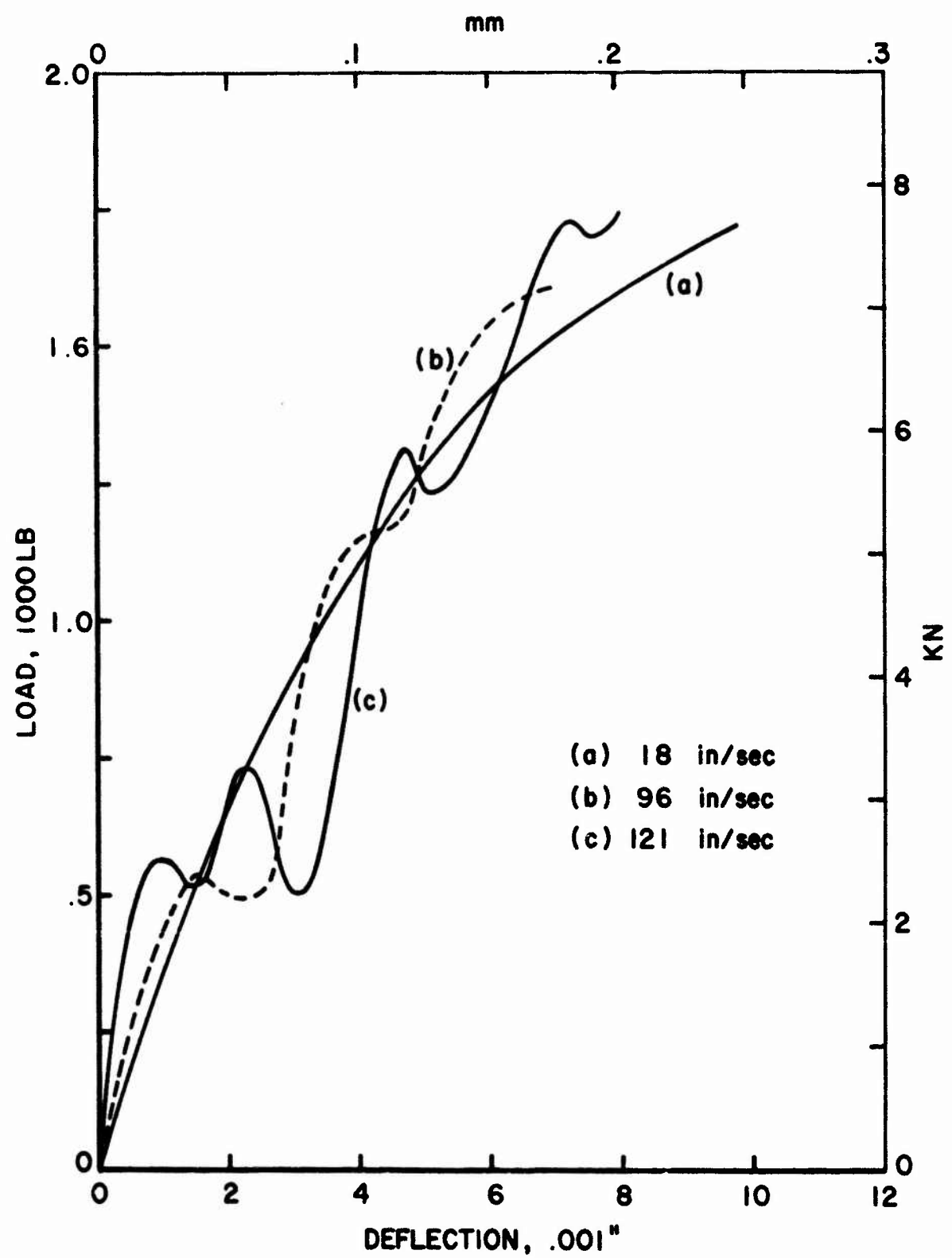


Figure 8. Typical Load-Deflection Curves for P-1 Beryllium

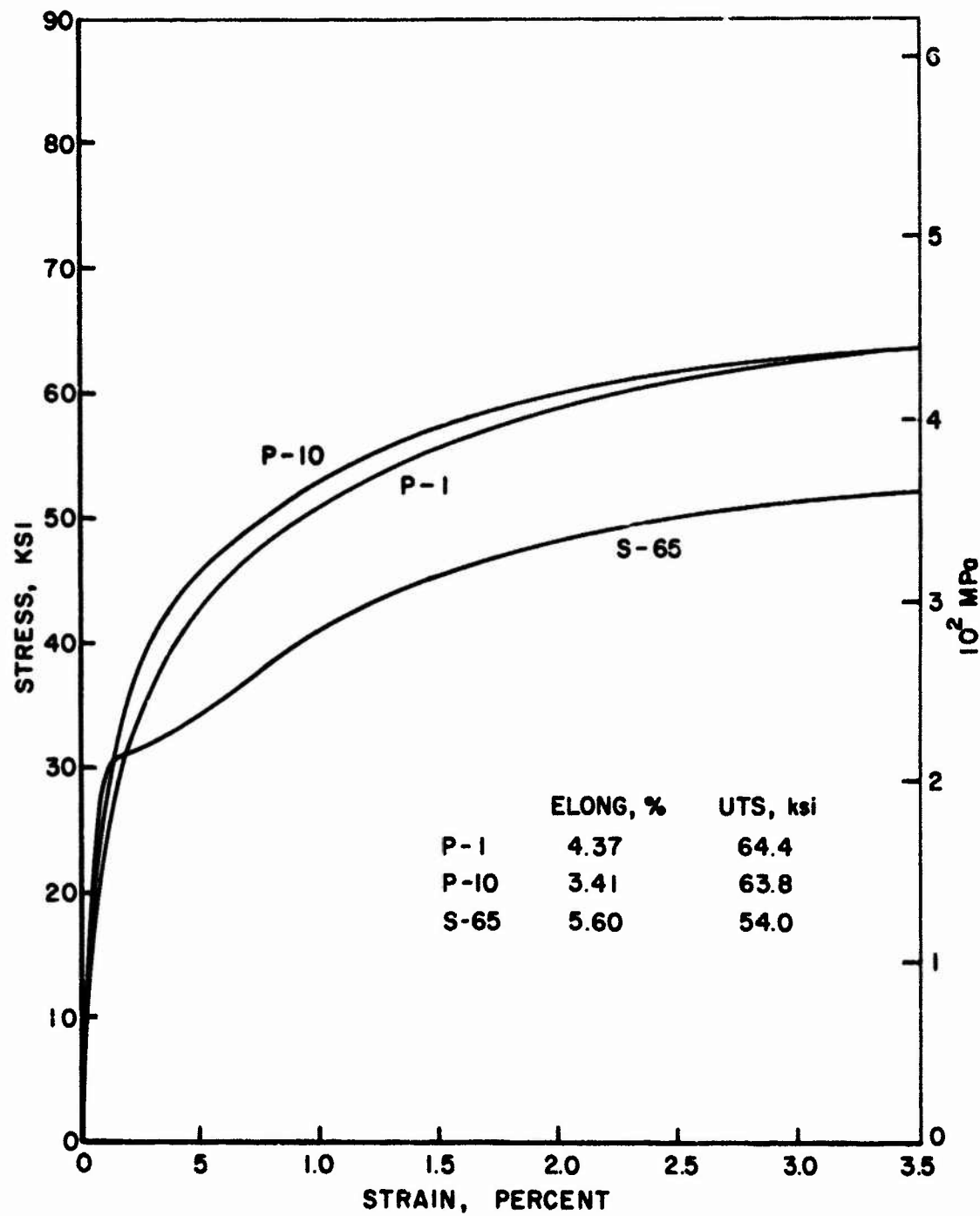


Figure 9. Uniaxial Stress-Strain Curves for Beryllium